

Effects of targeted muscle reinnervation on spinal cord motor neurons in rats following tibial nerve transection

<https://doi.org/10.4103/1673-5374.332153>

Wei Lu^{1,2}, Jian-Ping Li², Zhen-Dong Jiang², Lin Yang^{2,*}, Xue-Zheng Liu^{1,*}

Date of submission: February 22, 2021

Date of decision: September 22, 2021

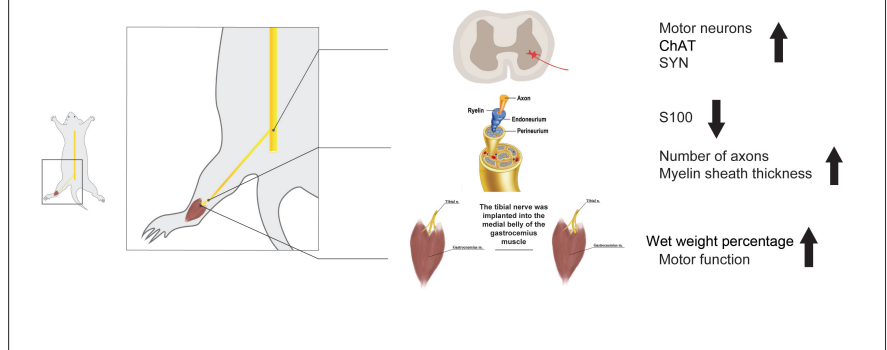
Date of acceptance: November 25, 2021

Date of web publication: January 7, 2022

From the Contents

Introduction	1827
Materials and Methods	1828
Results	1829
Discussion	1830

Graphical Abstract *Tibial nerve implanted into gastrocnemius muscle affects spinal cord motor neurons in rats*



Abstract

Targeted muscle reinnervation (TMR) is a surgical procedure used to transfer residual peripheral nerves from amputated limbs to targeted muscles, which allows the target muscles to become sources of motor control information for function reconstruction. However, the effect of TMR on injured motor neurons is still unclear. In this study, we aimed to explore the effect of hind limb TMR surgery on injured motor neurons in the spinal cord of rats after tibial nerve transection. We found that the reduction in hind limb motor function and atrophy in mice caused by tibial nerve transection improved after TMR. TMR enhanced nerve regeneration by increasing the number of axons and myelin sheath thickness in the tibial nerve, increasing the number of anterior horn motor neurons, and increasing the number of choline acetyltransferase-positive cells and immunofluorescence intensity of synaptophysin in rat spinal cord. Our findings suggest that TMR may enable the reconnection of residual nerve fibers to target muscles, thus restoring hind limb motor function on the injured side.

Key Words: function reconstruction; motor neuron; nerve injury; nerve implant; Nissl staining; spinal cord; synaptophysin; targeted muscle reinnervation; tibial nerve; transection

Introduction

Fitting prostheses is the primary method to help patients with an amputation to restore their limb function. The current commercial prostheses in China have disadvantages, as they are single function and provide only slow prosthetic control and, thus, clumsy movements (Fan et al., 2015; Kang et al., 2016). Achieving intuitive control of multifunctional prostheses is important for patients with a high level of amputation, so they can learn to use bionic artificial limbs intuitively. This, in turn, promotes motor function recovery and improves patients' quality of life (Loyalka et al., 2014; Krasoulis et al., 2020). The key to accomplishing intuitive control of multifunctional prostheses is by collecting the sources of the surface electromyogram (EMG) signals that are used for normal myoelectric prostheses (Wang et al., 2020). In recent years, studies have found that EMG signals collected from a residual limb of patients with an amputation can be used to calibrate prosthetic limb movements (Wilke et al., 2019; Williams et al., 2019; Krasoulis et al., 2020). Researchers record surface EMG signals generated by limb movements and decode the EMG signals to achieve normal prosthetic movements through motors; this is expected to provide multifunctional, intuitive bionic prostheses for patients with amputations (Hazubski et al., 2020). Unfortunately, after amputation, the source of neural information is

limited; a higher level of amputation leads to fewer remaining limb muscles and more limb movements that need to be restored (Kuiken et al., 2007).

Targeted muscle reinnervation (TMR) offers the possibility of reconstructing limb motor function and obtaining sufficient motor nerve information for people with disabilities (Kuiken et al., 2004). TMR is a novel neural-machine interface technology that involves the transfer of remaining peripheral nerves of an amputated limb into specific target muscles, allowing the target muscles to act as bioamplifiers to reconstruct the motor nerve information source lost after amputation (Kuiken et al., 1993; Hargrove et al., 2013). A previous study showed that TMR can successfully establish a connection between transplanted nerves and the target muscle, restore the transport of neurotrophic factors between nerve and muscle, and allow normal multifunctional myoelectric prostheses to intuitively provide potential sources of information (Wang et al., 2020). The regeneration rate of brachial plexus nerves transferred to pectoralis major muscles using TMR surgery is very slow (Huang et al., 2016), and the effect of TMR on the residual nerve fibers and motor neurons is still unclear. Therefore, this study aimed to investigate the effect of TMR surgery on injured motor neurons in the spinal cord of rats after tibial nerve transection (TNT).

¹Department of Human Anatomy, School of Basic Medical Sciences, Guangxi Medical University, Nanning, Guangxi Zhuang Autonomous Region, China;

²Department of Human Anatomy, Zhuhai Campus of Zunyi Medical University, Zhuhai, Guangdong Province, China

*Correspondence to: Xue-Zheng Liu, MD, 544758611@qq.com; Lin Yang, MD, iyzwill@aliyun.com.

<https://orcid.org/0000-0003-1372-8677> (Lin Yang)

Funding: The study was funded by the National Natural Science Foundation of China, Nos. 81760416, 81960419, 81927804 (all to LY), Science and Technology foundation of Guizhou Province, No. [2017]1226 (to LY), and Support Plan for High Level Talents in Guizhou High Education Institutions, No. KY[2018]056 (to LY).

How to cite this article: Lu W, Li JP, Jiang ZD, Yang L, Liu XZ (2022) Effects of targeted muscle reinnervation on spinal cord motor neurons in rats following tibial nerve transection. *Neural Regen Res* 17(8):1827-1832.

Materials and Methods

Experimental animals

Forty specific-pathogen-free (SPF) adult Sprague-Dawley rats, 20 male and 20 female, weighing 220 ± 20 g, were purchased from the Guangdong Medical Laboratory Animal Center, Guangzhou, China (license No. SCXK (Yue) 2013-0002). The rats were kept in an SPF environment at the Zhuhai campus of Zunyi Medical University, Zhuhai, China. The rats were housed in individual cages at a constant room temperature of $22 \pm 2^\circ\text{C}$ and relative humidity of 40–60% with a 12-hour dark/light cycle. The animals were randomly divided into four groups: normal control, TNT, TMR-6W (6 weeks after TMR surgery), and TMR-12W (12 weeks after TMR surgery), with ten rats in each group. The 40 Sprague-Dawley rats were randomly divided into the four groups using a random number table to avoid human factors affecting the experimental results. This study was approved by the Animal Ethics Committee of the Zhuhai campus of Zunyi Medical University, Zhuhai, China (approval No. 2019-2-273) on March 11, 2019. This study was reported in accordance with the ARRIVE 2.0 guidelines (Animal Research: Reporting of *In Vivo* Experiments) (Percie du Sert et al., 2020).

Surgical procedures

Rats were anesthetized with isoflurane (1.38–2.4% induction and 2.0–3.0% maintenance; Shenzhen Ruiwode Life Technology Co. Ltd., Shenzhen, China) using a gas anesthesia machine suitable for rats (RWD Life Science Co., Ltd., Shenzhen, China). The normal control group did not undergo surgery (Figure 1A and D) and had normal nerve and muscle structures. For the TNT group, the rats were fixed in the prone position on the operating table, and the hair from the gluteal region to the popliteal fossa of the left hind limb was shaved with hair-remover cream. At the popliteal fossa, a 1.5 cm longitudinal incision was made in the skin, and the subcutaneous fascia and muscles were separated bluntly until the tibial nerve was exposed. The target nerve and muscle (tibial nerve and gastrocnemius muscle and branches) were isolated, the tibial nerve and the medial and lateral heads of the gastrocnemius muscle were exposed using a glass hook and microsurgical instruments, and the tibial nerve and the motor branch to the medial head of the gastrocnemius muscle were transected with ophthalmic scissors (Shanghai Precision Instrument Co., Ltd., Shanghai, China) after ligation (Figure 1B and E). In the TMR group, the tibial nerve and the motor branch to the medial head of the gastrocnemius muscle were transected, and the proximal end of the transected tibial nerve was sewn over the medial belly of the gastrocnemius muscle using surgical instruments (Shanghai Medical Instruments Co. Ltd., Shanghai, China) and a surgical operating microscope (XT-X-4A, Zhenjiang Xintian Medical Devices Co., Ltd., Zhenjiang, China) (Figure 1C and F). After surgery, the skin was closed, and rats were returned to their cages and fed normally. The rats in the TMR-6W group were sacrificed 6 weeks after surgery and the gastrocnemius muscles, tibial nerves (0.5 cm from the point of nerve transection), and the lumbosacral enlargements of the spinal cords were removed for analysis.

Measurement of sciatic functional index

The sciatic functional index (SFI) is used to assess motor function recovery after sciatic nerve injury through gait analysis. SFI reflects the recovery of hind limb muscle strength and muscle coordination, and also evaluates the functional recovery of the sciatic nerve (Chen et al., 2020). The SFI data from the TMR-6W group were recorded 6 weeks after surgery. The SFI data from the normal control, TNT, and TMR-12W groups were recorded 12 weeks after surgery. A self-made footprint walking box lined with A4 white printer paper was used. Carbon ink was applied to the hind feet of rats, and they were allowed to walk freely in the box. Four to five clear footprints of each normal (N) and experimental (E) hind foot were recorded. The footprint length (PL), toe spread (TS), and inter-toe distance (IT; intermediary toe spread) were measured. These variables were entered into the Bain equation to calculate SFI, where 0 indicates normal and -100 indicates complete transection. $\text{SFI} = -38.3(\text{EPL} - \text{NPL}) / \text{NPL} + 109.5(\text{ETS} - \text{NTS}) / \text{NTS} + 13.3(\text{EIT} - \text{NIT}) / \text{NIT} - 8.8$.

The wet weight percentage of gastrocnemius muscle

To determine muscle atrophy after injury and indirectly assess nerve regeneration efficacy, we calculated the wet weight percentage of the gastrocnemius muscle on the operated side compared with the normal side for each group of rats. The lower the wet weight percentage of the gastrocnemius muscle, the greater the muscle atrophy. Both gastrocnemius muscles were removed completely at the muscle starting and ending points, the fat on the surface of the

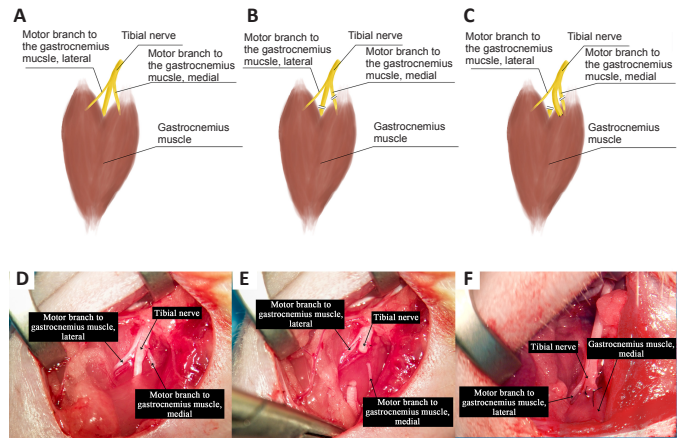


Figure 1 | Establishment of the left hind limb TNT and TMR models in rats (posterior view).

The left hind limb TMR model in Sprague-Dawley rats was established using a surgical operating microscope as described in the Materials and Methods section. (A–C) Schematic diagram of the left hind limb model in rats in the normal (A), TNT (B), and TMR (C) groups. (D–F) Surgical view of the left hind limb of rats. (D) The tibial nerve and its branches were exposed. (E) The tibial nerve and motor branch to the medial head of the gastrocnemius muscle were transected. (F) The proximal end of the transected tibial nerve was sewn over the medial belly of the gastrocnemius muscle. TMR: Targeted muscle reinnervation; TNT: tibial nerve transection.

muscles was peeled off, and the blood was wiped away with filter paper. Then, the gastrocnemius muscles were placed on an analytical balance (ESJ50-5A, Shanghai Precision Instrument Co., Ltd.) to obtain their wet weight. The wet weight percentage of the gastrocnemius muscles was determined by using the following equation: wet weight of operation side (left)/wet weight of normal side (right) \times 100.

Luxol fast blue staining of the tibial nerve

To show the morphological structures and pathological changes of the nerve myelin sheaths, luxol fast blue (LFB) staining was performed. The rats were anesthetized as above. Then, the tibial nerve was removed, fixed for 48 hours, and embedded in paraffin; paraffin sections were then cut with a microtome (RM 2016, Leica Instruments Ltd., Wetzlar, Germany). After deparaffinization, the sections were placed into LFB staining solution (Wuhan Servicebio Technology Co., Ltd., Wuhan, China) and stained overnight at 60°C in the dark for 12 hours. Then sections were rinsed in 95% alcohol to remove excess stain and rinsed three times in distilled water. The sections were differentiated in 0.05% lithium carbonate aqueous solution (Wuhan Servicebio Technology Co., Ltd.) for 15 seconds and then in 70% ethyl alcohol for another 30 seconds. The sections were dehydrated, cleared, mounted with neutral resin, and observed with an upright light microscope (ECLIPSE E100, Nikon, Tokyo, Japan). Serial transverse slides of the paraffin-embedded nerve tissue were obtained and analyzed at intervals of six sections. The slides were scanned using an upright microscope (ECLIPSE E100, Nikon) with a 40 \times objective lens. The number of axons was manually calculated in three non-overlapping areas ($100 \times 100 \mu\text{m}^2$).

Nissl staining of the spinal cord

We used Nissl staining to identify spinal cord motor neurons. A decrease in the number of Nissl bodies and abnormal motor neuron morphology indicated that nerve cells may be damaged. Paraffin sections of the lumbosacral enlargements of the spinal cord were deparaffinized and rehydrated, and the sections were stained with toluidine blue (Sinopharm Chemical Reagent Co., Ltd., Shanghai, China) for 5 minutes, washed with water, and differentiated with 1% glacial acetic acid (Sinopharm Chemical Reagent Co., Ltd.). The reaction was terminated with tap water. The degree of stain differentiation was controlled by observation under an upright microscope (ECLIPSE E100, Nikon). After washing with water, the sections were dried in an oven (Sinopharm Chemical Reagent Co. Ltd.), cleared with xylene for 5 minutes, and mounted with neutral gum (Sinopharm Chemical Reagent Co., Ltd.). Serial coronal slides of the paraffin-embedded lumbosacral enlargements of the spinal cord were obtained and analyzed at intervals of six sections. The section thickness was 5 μm . The slides were scanned using an upright microscope (ECLIPSE E100, Nikon) with a 40 \times objective lens. The

number of motor neurons in the lateral nucleus of the anterior horn of the spinal cord was manually calculated in three non-overlapping areas ($220 \times 350 \mu\text{m}^2$).

Immunohistochemical staining

Protein S100-B immunohistochemical staining was used to identify the myelin sheaths of tibial nerves. There are many cholinergic neurons in the spinal cord. Acetylcholine is a neurotransmitter used by all cholinergic neurons; thus, choline acetyltransferase (ChAT) is used as a marker of cholinergic neurons. The changes in ChAT activity and the number of ChAT-positive cells after spinal cord injury can reflect the functional status of nerve cells in the spinal cord (Petrova et al., 2015). In this study, anti-ChAT antibody immunohistochemical staining was used to specifically label motor neurons in the anterior horn of the spinal cord. Serial coronal slides of the paraffin-embedded tibial nerve or lumbosacral enlargements of the spinal cord were obtained and analyzed at intervals of six sections. Paraffin sections of the tibial nerve or lumbosacral enlargements of the spinal cord were deparaffinized and rehydrated to water. Sections were subjected to heat-induced antigen retrieval and cooled naturally, and endogenous peroxidase activity was blocked with 3% hydrogen peroxide (Sinopharm Chemical Reagent Co., Ltd.). Subsequently, sections were blocked with 3% bovine serum albumin at room temperature for 30 minutes and incubated with primary antibody at 4°C overnight in a humid box. The primary antibodies used were mouse anti-S100-B antibody to stain tibial nerves (1:2000, Cat# bsm-10832M, RRID:AB_2895151, Bioss, Woburn, MA, USA) or rabbit anti-ChAT antibody to stain spinal cords (1:400, Cat# bs-0042R, RRID:AB_10856836, Bioss). Sections were then incubated with horseradish peroxidase-conjugated rabbit secondary antibody from the ChemMate DAKO EnVision Detection Kit (1:1000, Cat# GK500705, RRID:AB_2895152, DAKO, Glostrup, Denmark) for 50 minutes at room temperature and developed with 3,3'-diaminobenzidine at room temperature. Thereafter, sections were counterstained with hematoxylin, washed with tap water, and differentiated in hematoxylin differentiation solution (Sinopharm Chemical Reagent Co., Ltd.) for 30 seconds. After washing with water, the sections were returned to blue with hematoxylin blue solution and were rinsed with running water. After dehydration and mounting, the sections were scanned using an upright microscope (ECLIPSE E100, Nikon) with a 40× objective lens. ImageJ (National Institutes of Health, Bethesda, MD, USA) (Schneider et al., 2012) was used to measure the average optical density of S100-B in the tibial nerve and ChAT in the lateral anterior horn of the spinal cord.

Immunofluorescence staining

Synaptophysin (SYN) is a protein localized to synaptic vesicles; its expression is closely associated with the transport of synaptic vesicles and the release of neurotransmitters (Thiel, 1993). Serial coronal slides of the paraffin-embedded lumbosacral enlargements of the spinal cord tissue blocks were obtained and analyzed at intervals of six sections. Paraffin sections of the lumbosacral enlargements of the spinal cord of rats in each group were deparaffinized, rehydrated to water, and subjected to antigen retrieval. The sections were quenched with autofluorescence quencher (Abcam, Cambridge, UK) for 5 minutes and washed with running water for 10 minutes. Thereafter, sections were blocked with bovine serum albumin blocking buffer for 30 minutes, incubated with rabbit anti-SYN antibody (1:500, Cat# bs-23504R, RRID:AB_2895150, Bioss) at 4°C overnight in a humid box, and incubated with goat anti-rabbit IgG/Cy3 antibody (1:500, Cat# bs-0295G-Cy3, RRID:AB_10892956, Bioss) for 50 minutes at room temperature. After nuclear counterstaining with 4',6-diamidino-2-phenylindole (Abcam) for 10 minutes, the sections were mounted with antifluorescence quenching medium (Abcam) and observed under an inverted fluorescence microscope (Eclipse Ti-SR, Nikon) using a 40× objective lens. ImageJ (National Institutes of Health) (Schneider et al., 2012) was used to measure the average optical density of SYN immunoreactivity in the lateral anterior horn of the spinal cord.

Statistical analysis

No statistical methods were used to predetermine sample sizes; however, our sample sizes are similar to those reported in a previous publication (Chen et al., 2020). No animals or data points were excluded from the analysis. SFI and histological analyses were conducted blinded. All data are expressed as the mean \pm standard deviation (SD). One-way analysis of variance followed by Bonferroni's multiple comparisons test was performed using GraphPad Prism version 6.0.0 for Windows (GraphPad Software, San Diego, California

USA, www.graphpad.com). The axon number data were normally distributed and the variances were unequal, so Welch's *t*-test was used to analyze the difference of distribution in four groups for axon number and myelin sheath thickness in rat tibial nerves. The variances were equal for the remaining data, so one-way analysis of variance with *post hoc* Bonferroni correction was performed for comparisons between multiple groups. A value of $P < 0.05$ was considered statistically significant.

Results

General conditions of rats

All rats drank and ate normally, the surgical wounds were free from infection and ulceration, and no signs of neurological disorders were observed.

Effect of TMR surgery on the recovery of motor function in rats

Gait analysis of rats in the normal control group showed clear footprints (Figure 2). At week 6, the SFI values of the TNT group were significantly lower than the normal group ($P < 0.05$), while the SFI values of the TMR group were significantly higher than the TNT group and were significantly lower than the normal group ($P < 0.05$; Figure 2E). At week 12, the SFI values of the TNT group were also significantly lower than the normal group ($P < 0.05$; Figure 2E), and the SFI values of the TMR group were significantly higher than the TNT group, which was still significantly lower than the normal group ($P < 0.05$; Figure 2E). In addition, the SFI values were similar at 6 weeks and 12 weeks in rats from the TMR group.

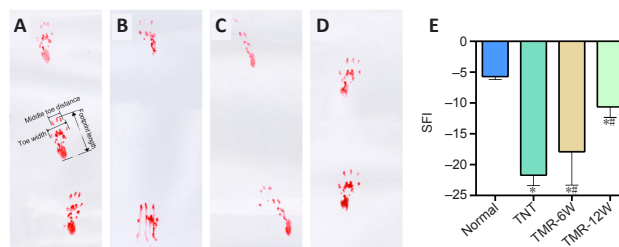


Figure 2 | Footprints from the left hind limb (injured side) in rats.

Motor function recovery after sciatic nerve injury was assessed through gait analysis using the sciatic function index (SFI) in the normal (A), TNT (B), TMR-6W (C), and TMR-12W (D) groups. Clear footprints of rats in the normal group were recorded. (E) At 6 and 12 weeks, the SFI of the TNT and TMR groups was significantly lower than the normal group, whereas the SFI of the TMR group was significantly higher than the TNT group. Data are expressed as the mean \pm SD. $n = 10$. * $P < 0.05$, vs. normal group; # $P < 0.05$, vs. TNT group (one-way analysis of variance with *post hoc* Bonferroni correction). SFI: Sciatic functional index; TNT: tibial nerve transection; TMR: targeted muscle reinnervation; 6W: 6 weeks; 12W: 12 weeks; SD: standard deviation.

Effects of TMR surgery on the wet weight percentages of gastrocnemius muscles of rats

As shown in Figure 3, the wet weight percentages of gastrocnemius muscles were significantly lower in the TNT, TMR-6W, and TMR-12W groups than in the normal group ($P < 0.05$). The gastrocnemius muscle wet weight percentages on the operated side were also significantly higher in the TMR-6W and TMR-12W groups compared with the TNT group ($P < 0.05$). No statistically significant differences in the gastrocnemius muscle wet weight percentages were observed between the TMR-6W and TMR-12W groups ($P > 0.05$).

Effects of TMR surgery on the number of axons and myelin sheath thickness in the tibial nerves of rat

Compared with the normal group, axon numbers were significantly decreased in the TNT group ($P < 0.05$; Figure 4A–I). In comparison with the TNT group, axon numbers were significantly increased in the TMR-6W and TMR-12W groups ($P < 0.05$). There was no statistically significant difference in axon numbers between the TMR-6W and TMR-12W groups ($P > 0.05$; Figure 4A–I).

Compared with the normal group, the myelin sheath was significantly thinner in the TNT group ($P < 0.05$; Figure 4A–H, J) and in the TMR-6W and TMR-12W groups ($P < 0.05$; Figure 4A–H, J). However, 12 weeks after TMR, the myelin sheath was significantly thicker in the TMR-12W group than in the TNT group ($P < 0.05$).

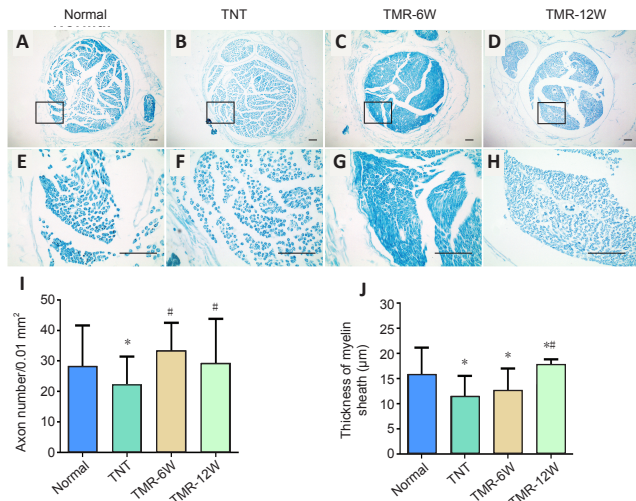
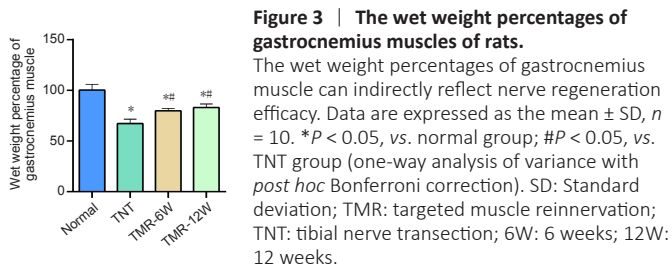


Figure 4 | Number of axons and myelin sheath thickness in the tibial nerve in rats.

(A–D) Representative LFB staining images of nerve cross sections from the normal, TNT, TMR-6W, and TMR-12W groups. (E–H) Higher magnification images of the black boxes in A–D. Blue areas are tissue sections stained with LFB staining solution. Scale bars: 50 μ m. Measurement data are shown on histograms I and J. (I) The number of axons per unit area. (J) Myelin sheath thickness. Data are expressed as the mean \pm SD, $n = 3$. * $P < 0.05$, vs. normal group; # $P < 0.05$, vs. TNT group (Welch's *t*-test). LFB: Luxol fast blue; TNT: tibial nerve transection; TMR: targeted muscle reinnervation; 6W: 6 weeks; 12W: 12 weeks; SD: standard deviation.

Effects of TMR surgery on S100-B immunoreactivity in the tibial nerves of rats

S100-B immunoreactivity on the operated side of rats was significantly increased in the TNT group compared with the normal group ($P < 0.05$) and was significantly decreased in the TMR-6W and TMR-12W groups compared with the TNT group ($P < 0.05$; **Figure 5**).

Effects of TMR surgery on spinal cord motor neurons in rats

The number of motor neurons was significantly lower in the TNT group than in the normal group ($P < 0.05$; **Figure 6**). The number of motor neurons was significantly higher in the TMR-6W group than in the TNT group ($P < 0.05$). In comparison with the TMR-6W group, the number of motor neurons in the TMR-12W group was increased, but there was no statistically significant difference between the two groups ($P > 0.05$; **Figure 6**).

The ChAT-positive cells were arranged in a disordered manner, and the number of cholinergic neurons were significantly reduced in the TNT group compared with the normal group ($P < 0.05$, **Figure 7I**). ChAT immunoreactivity was also significantly decreased in the TNT group compared with the normal group ($P < 0.05$). In comparison with the TNT group, the number of cholinergic neurons in the spinal cord was significantly increased ($P < 0.05$) and ChAT immunoreactivity was significantly enhanced ($P < 0.05$; **Figure 7J**) in the TMR-6W and TMR-12W groups.

Effects of TMR surgery on synaptophysin expression in spinal cord motor neurons in rats

Immunofluorescence staining revealed strong SYN immunoreactivity in motor neurons in the anterior horn of the spinal cord of rats in the normal group. Compared with the normal group, SYN-positive cells

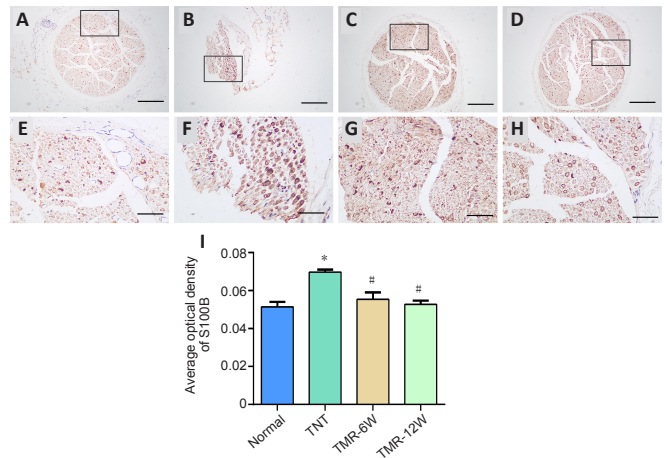


Figure 5 | Expression of S100-B (a marker for myelin sheaths of nerves) on the operated side of rats.

Representative S100-B immunohistochemical staining images in the normal (A), TNT (B), TMR-6W (C), and TMR-12W (D) groups; E–H are enlarged views of the local areas in A–D. Scale bars: 200 μ m in A–D, 50 μ m in E–H. (I) Average optical density of S100-B. Data are expressed as the mean \pm SD, $n = 3$. * $P < 0.05$, vs. normal group; # $P < 0.05$, vs. TNT group (one-way analysis of variance with *post hoc* Bonferroni correction). TNT: Tibial nerve transection; TMR: targeted muscle reinnervation; 6W: 6 weeks; 12W: 12 weeks; SD: standard deviation.

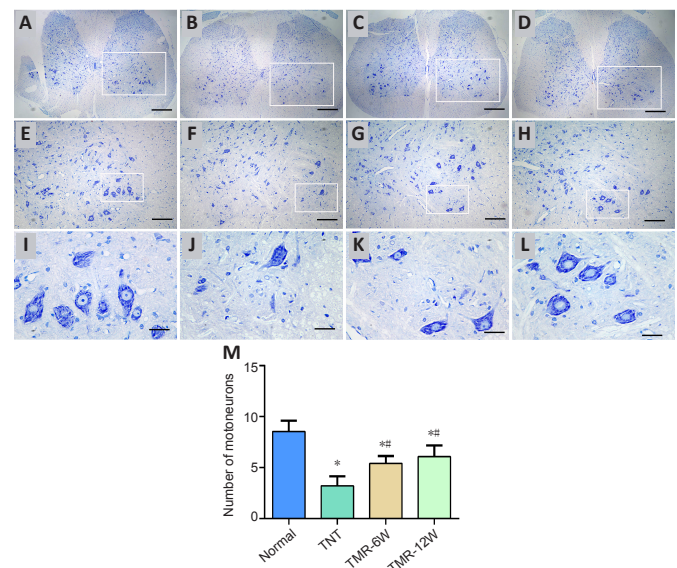


Figure 6 | Nissl staining of cross sections from the lumbosacral enlargements of the spinal cords of rats.

(A) In the normal group, there were large numbers of mainly large- and medium-sized anterior horn motor neurons that were tightly arranged. Abundant Nissl bodies were observed, the cell bodies and nuclei were clearly visible, and the axons and dendrites were easily distinguished. (B) In the TNT group, a scattered arrangement of neurons was observed, with few large- and medium-sized neurons. The cell bodies were small and the Nissl bodies were blurred. (C, D) In the TMR-6W (C) and TMR-12W (D) groups, motor neurons were densely arranged, and many large neurons were visible, with their cytoplasm uniformly stained. E–H are enlarged views of the local areas in A–D; I–L are enlarged views of the local areas in E–H. Scale bars: 500 μ m in A–D, 200 μ m in E–H, and 50 μ m in I–L. (M) The number of anterior horn motor neurons. Data are expressed as the mean \pm SD, $n = 3$. * $P < 0.05$, vs. normal group; # $P < 0.05$, vs. TNT group (one-way analysis of variance with *post hoc* Bonferroni correction). TNT: Tibial nerve transection; TMR: targeted muscle reinnervation; 6W: 6 weeks; 12W: 12 weeks; SD: standard deviation.

were arranged in a disordered manner and SYN immunoreactivity was significantly reduced in the TNT group ($P < 0.05$; **Figure 8**). Compared with the TNT group, SYN immunoreactivity in motor neurons in the anterior horn of the spinal cord was significantly enhanced in the TMR-6W and TMR-12W groups ($P < 0.05$; **Figure 8**).

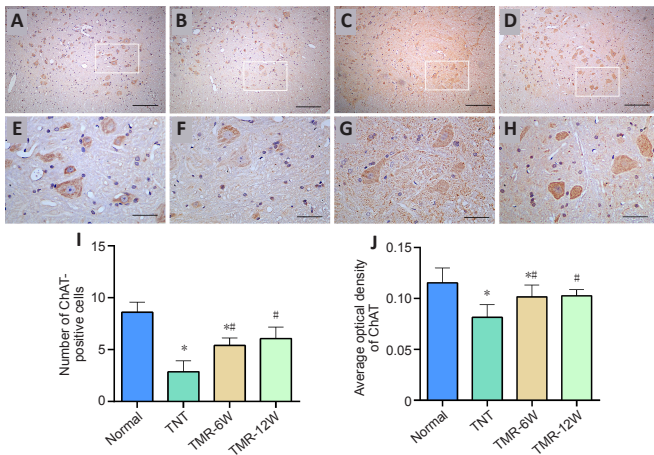


Figure 7 | Choline acetyltransferase immunoreactivity in the spinal cords of rats.

Representative immunohistochemical staining images of ChAT in the normal (A), TNT (B), TMR-6W (C), and TMR-12W (D) groups; E–H are enlarged views of the local areas in A–D. Scale bars: 200 μm in A–D, 50 μm in E–H. (I) The number of ChAT-positive neurons in the anterior horn of the spinal cord. The cell numbers were significantly reduced in the TNT group compared with the normal group. The number of cholinergic neurons in the spinal cord was significantly increased in the TMR-6W and TMR-12W groups compared with the TNT group. (J) Average optical density of ChAT. ChAT expression was significantly decreased in the TNT group compared with the normal group. ChAT expression was significantly enhanced in the TMR-6W and TMR-12W groups compared with the TNT group. Data are expressed as the mean ± SD, $n = 3$. * $P < 0.05$, vs. normal group; # $P < 0.05$, vs. TNT group (one-way analysis of variance with *post hoc* Bonferroni correction). ChAT: Choline acetyltransferase; TNT: tibial nerve transection; TMR: targeted muscle reinnervation; 6W: 6 weeks; 12W: 12 weeks; SD: standard deviation.

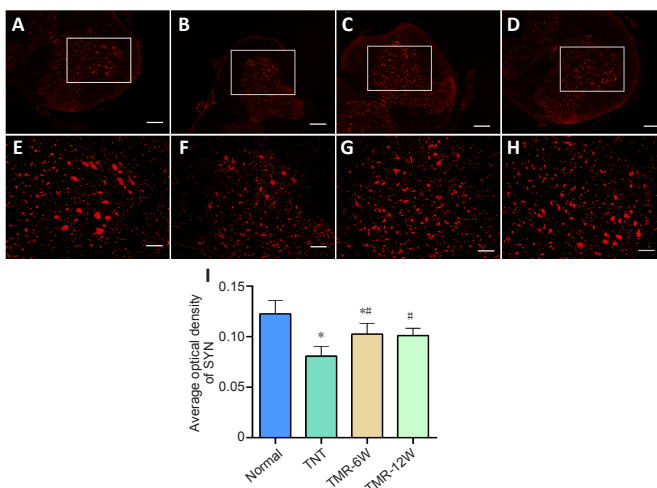


Figure 8 | Synaptophysin expression in motor neurons in the anterior horn of the spinal cord in rats.

Representative immunofluorescence staining images of SYN in the normal (A), TNT (B), TMR-6W (C), and TMR-12W (D) groups; E–H are enlarged views of the local areas in A–D. Scale bars: 200 μm in A–D, 50 μm in E–H. (I) Average optical density of SYN. Data are expressed as the mean ± SD, $n = 3$. * $P < 0.05$, vs. normal group; # $P < 0.05$, vs. TNT group (one-way analysis of variance with *post hoc* Bonferroni correction). SYN: Synaptophysin; TNT: tibial nerve transection; TMR: targeted muscle reinnervation; 6W: 6 weeks; 12W: 12 weeks; SD: standard deviation.

Discussion

TMR is a surgical procedure used to transfer residual peripheral nerves from amputated limbs to targeted muscles, allowing the target muscles to become sources of motor control information for function reconstruction. TMR after upper-extremity amputation can effectively reconstruct muscle and nerve function (Huang et al., 2016); subsequent low-frequency electrical stimulation and treadmill training have a positive effect on generation of connections between

the target muscles and transplanted nerves (Zhang et al., 2015). However, the effect of TMR on the fibers and cell bodies of injured motor neurons is still unclear, so it is important to establish a suitable TMR model to study this effect. In this study, we transected the tibial nerve and medial head of the gastrocnemius muscle and transferred the proximal end of the transected tibial nerve into the medial belly of the gastrocnemius muscle to establish a rat hind limb TMR model. Because the tibial nerve is thick and the medial head of the gastrocnemius muscle is located superficially, this method gives the advantage of allowing us to easily analyze the effect of TMR on motor neurons and to use a less traumatic surgical technique; this model reduces the chance of muscle atrophy caused by surgical trauma and facilitates nerve reconstruction of the muscle. In this study, we transected the medial head of the gastrocnemius muscle to reduce the original innervation of the gastrocnemius muscle; this is beneficial to determine the trophic effect of TMR on denervated muscles.

Our study showed that significant denervation atrophy was observed in the target gastrocnemius muscle after TNT. This result is consistent with the finding of a previous study (Weng et al., 2018). Moreover, we observed a relationship between reduced muscle atrophy of the gastrocnemius muscle and TMR. This suggests that the residual nerve may have established an effective connection with the target muscle, which may be the main reason for partial recovery of motor function. In addition, we noticed that, over a longer time period (12 weeks), the SFI values and gastrocnemius muscle wet weight percentages on the operated side in the TMR group did not reach the levels observed in the normal group, reflecting partial recovery of motor function.

TNT is a severe nerve injury, as nerve trunk continuity is destroyed. The residual fiber can undergo retrograde degeneration due to ischemic nerve inflammation and edema (Wang et al., 2006). The neurotrophic factors from the cell bodies at the residual end of the nerve are upregulated in response to injury, which can promote the regeneration of axons (Marshall and Farah, 2021). However, the nerve regeneration is slow, and the speed of Wallerian degeneration is faster than nerve regeneration (Conforti et al., 2014; Girouard et al., 2018). The status of the proximal nerve cell bodies is also an important factor for neuronal survival and regeneration. The protective effect of TMR on residual fibers is unclear. The morphological characteristics of peripheral nerves can be evaluated in terms of the number of axons in nerve cross sections and the morphological changes in the myelin sheath. In this study, we measured the changes in myelin sheath thickness of the peripheral nerve and the number of neuronal axons wrapped in the myelin sheaths using LFB staining. Our results showed that the number of axons was significantly lower and myelin sheath thickness was thinner in rats undergoing TNT than in rats in the normal group. This result is consistent with a previous study investigating another peripheral nerve injury model (Wang et al., 2013), which further confirms our successful establishment of the TNT model. At 6 weeks after TMR, axon numbers were restored to normal, with no statistically significant difference found between TMR and normal groups. Myelin sheath thickness was improved after 12 weeks of TMR but had not fully returned to normal. Our results indicate that TMR may initiate faster repair of neurons than glial cells, but the impact of this aspect has been rarely studied thus far. Therefore, we are interested in addressing in our future research whether we can improve the rate of neural regeneration by simultaneously increasing the rate of myelin regeneration.

Schwann cells are the main cells that cause changes in protein expression at the injured site, which can promote the release of neurotrophic factors such as nerve growth factor and ciliary neurotrophic factor, and that maintain the microenvironment to promote axon regeneration (Kim et al., 2019). The expression levels of S100-B are positively correlated with the severity of neurological disorders such as acute brain injury, brain tumors, and neurodegenerative diseases (Itoyama et al., 2020; Yang et al., 2020). In this study, we found that S100-B expression in the myelin sheaths of residual fibers was significantly increased after TNT, suggesting that the microenvironment is not conducive for Schwann cells to be converted to promote axonal regeneration after transection, which results in further nerve fiber degeneration. After the residual tibial nerve stump was transposed into the medial head of the gastrocnemius muscle, we found that S100-B expression in the residual tibial nerve was significantly downregulated, suggesting that TMR surgery may improve the microenvironment of nerve fibers to promote nerve regeneration. TNT completely blocks the transport of neurotrophic factors between the nerve and muscle, causing accumulation of large amounts of anterogradely transported materials in the nerve stump,

which seriously affects normal nerve repair (Soendenbroe et al., 2019). After the tibial nerve stump is transposed into the target muscle, the neuromuscular junction is established and material transport resumes, which may be important for TMR to improve the microenvironment and promote the survival of nerve fibers.

Peripheral nerve injuries or transection injuries lead to the destruction of myelin sheaths, disintegration of the axonal cytoskeleton, and axonal swelling through retrograde degeneration, leading to the death of neurons in the injured area (Giorgetti et al., 2019; Liu and Wang, 2020). ChAT is the rate-limiting enzyme in acetylcholine synthesis; the functional status of motor neurons can be measured by the expression levels of ChAT. In this study, cross sections from the lumbosacral enlargements of the spinal cord were stained for reactivity to Nissl and ChAT using immunohistochemistry methods. The results showed that the number of motor neurons and Nissl bodies and ChAT expression levels in the anterior horn of the spinal cord on the injured side were significantly reduced after TNT. The decrease in the number of Nissl bodies and ChAT expression levels indicates that TNT causes a stress state in the cell bodies of motor neurons and a significant decrease in protein synthesis in motor neurons, which may destroy the stability of the intracellular environment and trigger a series of immune responses, ultimately leading to neuronal apoptosis (Silman et al., 2008). In this study, we found that the number of anterior horn motor neurons and Nissl bodies were significantly increased and ChAT expression was upregulated in the TMR group compared with the TNT group, indicating that the tibial nerve stumps established new connections with the target muscles in the TMR surgery group. These new connections may improve the intracellular environment of motor neurons in the anterior horn of the spinal cord, which is conducive to the survival of the anterior horn motor neurons.

SYN is a protein localized to synaptic vesicles. Synaptic vesicles are present in presynaptic terminals of neurons. They participate in the release of activity-dependent neurotransmitters and play an irreplaceable role in the process of synaptic plasticity. Our results showed that SYN expression was significantly reduced in the TNT group compared with the normal group, suggesting that TNT may damage the protein synthesis function of motor neurons in the anterior horn of the spinal cord. Significant restoration of SYN levels was observed in the TMR-6W and TMR-12W groups but not in the TNT group. TMR surgery may improve the intracellular environments of nerve cell bodies, thus enhancing neuron survival.

Limitations

These experiments have some limitations. Firstly, we observed that TMR surgery protects motor neuron survival, but we did not explore the molecular mechanisms behind this protection. Secondly, animal experiments and clinical applications may give different results, and we should investigate the effects of TMR in a clinical research setting.

Conclusions

In this study, we successfully established a hind limb TMR model in Sprague-Dawley rats. Our findings show that the TMR technique enables the reconnection of residual nerve fibers with the target muscle, restores motor function in the hind limb on the injured side, and improves the microenvironment for the survival of residual nerve fibers and neuronal cell bodies, leading to reinnervation of hind limb muscles. We still need to explore the mechanisms that regulate the protective effect of TMR on motor neuron survival. In future studies, we will continue to explore rehabilitation methods or drugs that can better promote motor function recovery after TMR.

Acknowledgments: *The authors would like to thank the Key Laboratory of Human-Machine-Intelligence Synergic System, Shenzhen Institutes of Advanced Technology, Chinese Academy of Sciences, Chinese Academy of Sciences-Guangdong-Hong Kong-Macao Joint Laboratory of Human-Machine Intelligence-Synergy Systems for their technical assistance.*

Author contributions: *XZL, LY, and WL conceived the project; WL established the animal models and collected the data; JPL and ZDJ analyzed the data; WL wrote the paper with help from all other authors. All authors approved the final version of the paper.*

Conflicts of interest: *The authors declare that there are no conflicts of interest associated with this manuscript.*

Open access statement: *This is an open access journal, and articles are distributed under the terms of the Creative Commons AttributionNonCommercial-ShareAlike 4.0 License, which allows others to remix, tweak, and build upon the work non-commercially, as long as appropriate credit is given and the new creations are licensed under the identical terms.*

©Article author(s) (unless otherwise stated in the text of the article) 2022. All rights reserved. No commercial use is permitted unless otherwise expressly granted.

References

- Chen ZX, Lu HB, Jin XL, Feng WF, Yang XN, Qi ZL (2020) Skeletal muscle-derived cells repair peripheral nerve defects in mice. *Neural Regen Res* 15:152-161.
- Conforti L, Gilley J, Coleman MP (2014) Wallerian degeneration: an emerging axon death pathway linking injury and disease. *Nat Rev Neurosci* 15:394-409.
- Fan H, Fu J, Li X, Pei Y, Li X, Pei G, Guo Z (2015) Implantation of customized 3-D printed titanium prosthesis in limb salvage surgery: a case series and review of the literature. *World J Surg Oncol* 13:308.
- Giorgetti E, Obrecht M, Ronco M, Panesar M, Lambert C, Accart N, Doelemeyer A, Nash M, Bidinosti M, Beckmann N (2019) Magnetic resonance imaging as a biomarker in rodent peripheral nerve injury models reveals an age-related impairment of nerve regeneration. *Sci Rep* 9:13508.
- Girouard MP, Bueno M, Julian V, Drake S, Byrne AB, Fournier AE (2018) The molecular interplay between axon degeneration and regeneration. *Dev Neurobiol* 78:978-990.
- Hargrove LJ, Simon AM, Young AJ, Lipschutz RD, Finucane SB, Smith DG, Kuiken TA (2013) Robotic leg control with EMG decoding in an amputee with nerve transfers. *N Engl J Med* 369:1237-1242.
- Hazubski S, Hoppe H, Otte A (2020) Electrode-free visual prosthesis/exoskeleton control using augmented reality glasses in a first proof-of-technical-concept study. *Sci Rep* 10:16279.
- Huang JP, Li WQ, Yang L, Zhu MX, Zhu XD, Li CY, Yang ZJ, Li GL (2016) A pilot study of nerve function reinnervation on a transhumeral amputee. *J Integr Technol* 5:30-37.
- Itoyama T, Yoshida S, Tomokiyo A, Hasegawa D, Hamano S, Sugii H, Ono T, Fujino S, Maeda H (2020) Possible function of GDNF and Schwann cells in wound healing of periodontal tissue. *J Periodontol Res* 55:830-839.
- Kim M, Kim H, Kim D, Kim D, Huh Y, Park C, Chung HJ, Jung J, Jeong NY (2019) Heme oxygenase 1 in schwann cells regulates peripheral nerve degeneration against oxidative stress. *ASN Neuro* 11:1759091419838949.
- Krasoulis A, Vijayakumar S, Nazarpour K (2020) Multi-grip classification-based prosthesis control with two EMG-IMU sensors. *IEEE Trans Neural Syst Rehabil Eng* 28:508-518.
- Kuiken TA, Childress DS, Rymer WZ (1995) The hyper-reinnervation of rat skeletal muscle. *Brain Res* 676:113-123.
- Kuiken TA, Dumanian GA, Lipschutz RD, Miller LA, Stubblefield KA (2004) The use of targeted muscle reinnervation for improved myoelectric prosthesis control in a bilateral shoulder disarticulation amputee. *Prosthet Orthot Int* 28:245-253.
- Kuiken TA, Miller LA, Lipschutz RD, Lock BA, Stubblefield K, Marasco PD, Zhou P, Dumanian GA (2007) Targeted reinnervation for enhanced prosthetic arm function in a woman with a proximal amputation: a case study. *Lancet* 369:371-380.
- Liu Y, Wang H (2020) Peripheral nerve injury induced changes in the spinal cord and strategies to counteract/enhance the changes to promote nerve regeneration. *Neural Regen Res* 15:189-198.
- Loyalca P, Liu L, Chen G, Zheng X (2014) The cost of disability in China. *Demography* 51:97-118.
- Marshall KL, Farah MH (2021) Axonal regeneration and sprouting as a potential therapeutic target for nervous system disorders. *Neural Regen Res* 16:1901-1910.
- Percie du Sert N, Ahluwalia A, Alam S, Avey MT, Baker M, Browne WJ, Clark A, Cuthill IC, Dirnagl U, Emerson M, Garner P, Holgate ST, Howells DW, Hurst V, Karp NA, Lázic SE, Lidster K, MacCallum CJ, Macleod M, Pearl EJ, et al. (2020) Reporting animal research: Explanation and elaboration for the ARRIVE guidelines 2.0. *PLoS Biol* 18:e3000411.
- Petrova ES, Kolos EA, Korzhovskii DE (2015) Differentiation of cholinergic neurons in rat spinal cord under conditions of allotransplantation into a peripheral nerve and in situ development. *Bull Exp Biol Med* 160:141-147.
- Schneider CA, Rasband WS, Eliceiri KW (2012) NIH Image to ImageJ: 25 years of image analysis. *Nat Methods* 9:671-675.
- Silman I, Sussman JL (2008) Acetylcholinesterase: how is structure related to function? *Chem Biol Interact* 175:3-10.
- Soendenbroe C, Heisterberg MF, Schjerling P, Karlens A, Kjaer M, Andersen JL, Mackey AL (2019) Molecular indicators of denervation in aging human skeletal muscle. *Muscle Nerve* 60:453-463.
- Thiel G (1993) Synapsin I, synapsin II, and synaptophysin: marker proteins of synaptic vesicles. *Brain Pathol* 3:87-95.
- Wang AL, Yuan M, Neufeld AH (2006) Degeneration of neuronal cell bodies following axonal injury in Wld(S) mice. *J Neurosci Res* 84:1799-1807.
- Wang CH, Wang B, Wendu RL, Bi HE, Cao GF, Ji C, Jiang Q, Yao J (2013) Protective role of Wallerian degeneration slow (Wld(s)) gene against retinal ganglion cell body damage in a Wallerian degeneration model. *Exp Ther Med* 5:621-625.
- Wang P, Li YH, Zhang ZJ, Lin YF, Jiang ZD, Ding XF, Yang L (2020) Effects of functional electrical stimulation on neuromuscular function after targeted muscle reinnervation surgery in rats. *Annu Int Conf IEEE Eng Med Biol Soc* 2020:3823-3826.
- Weng J, Wang YH, Li M, Zhang DY, Jiang BG (2018) GSK3beta inhibitor promotes myelination and mitigates muscle atrophy after peripheral nerve injury. *Neural Regen Res* 13: 324-330.
- Wilke MA, Niethammer C, Meyer B, Farina D, Dosen S (2019) Psychometric characterization of incidental feedback sources during grasping with a hand prosthesis. *J Neuroeng Rehabil* 16:155.
- Williams HE, Boser QA, Pilarsk PM, Chapman CS, Vette AH, Hebert JS (2019) Hand function kinematics when using a simulated myoelectric prosthesis. *IEEE Int Conf Rehabil Robot* 2019:169-174.
- Yang X, Ji C, Liu X, Zheng C, Zhang Y, Shen R, Zhou Z (2020) The significance of the neuregulin-1/ErbB signaling pathway and its effect on Sox10 expression in the development of terminally differentiated Schwann cells in vitro. *Int J Neurosci* 1:1-10.
- Zhang L, Zhou H, Yang L, Huang J, Yang W, Li G (2015) Effects of low frequency electrical stimulation in targeted muscle reinnervation rat model. *Zhongguo Kangfu Yixue Zazhi* 30:3-9,54.